

Confinement of Polysoaps in Nonionic Surfactant Lyotropic Bilayers

Y. Yang¹, R. Prud'homme¹, P. Richetti², and C. M. Marques²

¹Department of Chemical Engineering, Princeton University,
Princeton, NJ 08544

²Rhodia/CNRS Complex Fluids Laboratory, Prospect Plains Road,
Cranbury, NJ 08512-7500

We study the confinement of hydrophobically modified polyacrylate (HMPA) in lamellar (L_α) and sponge (L_3) phases of a ternary lyotropic system, comprising n-dodecyl pentaethylene glycol monoether ($C_{12}EO_5$), hexanol and brine. The unmodified polymer cannot be inserted into the membrane solution, but the confinement of HMPA can be achieved with a sufficient amount of hydrophobe substitution. The resulting stapled polymer structure induces pronounced changes in the phase behavior of the surfactant solution as well as in the membrane properties. Neutron scattering and visual observation were used to obtain phase diagrams and information on membrane properties. We found that the confinement of HMPA 1) induces two new phases: a vesicle-like phase and two coexisting L_α phases, 2) reduces the monophasic L_α area, and 3) increases the rigidity of the bilayers. The effects of the hydrophobe substitution level and polymer concentration are systematically explored.

Adding polymer into a membrane solution results in changes of both the properties of individual membrane and the inter-membrane interactions. For instance, the smectic compression modulus, \bar{B} , or the average spacing distance, d , are functions of the membrane flexibility, that can be changed by the presence of the polymers. Accordingly, new phase regions may appear in the phase diagram. Industrially, polymer-membrane complexes are of importance in the formulation of liquid detergents and cosmetics. In the biological realm, the walls of liposomes and cells are built from phospholipid bilayers that anchor a variety of macromolecular species. Understanding the structure/property relationships for polymer/membrane systems would be a step towards the of polymer architectures to create or enhance a desired phase structure, rheological property, or vesicle stability.

Ionic or nonionic membranes have different interactions with polymers. For example, an ionic lamellar phase can confine a non-charged polymer with the radius of gyration several times larger than the interlayer spacing [1]. In contrast, polymers create phase separation in nonionic surfactant mesophases [2-6]. Miscibility between dissolved polymers and non-ionic surfactant mesophases can, nevertheless, be achieved by grafting hydrophobic side groups onto the backbone: the hydrophobic side chains anchor the polymer to the lyotropic membrane [2-7]. The variation of the bending modulus, κ , the Gaussian bending modulus, $\bar{\kappa}$, and the compression modulus, \bar{B} , upon adding polymers has been theoretically and experimentally studied [8-13]. Polymer induced excess membrane rigidity from an anchoring polymer system was recently reported by our group [14].

This paper focuses on the lamellar L_α phase consisting of one-dimensional stacks of surfactant bilayers separated by a solvent. The sponge phase L_3 , a bicontinuous isotropic phase of multiconnected membranes [15] is also studied. We systematically investigate the effect of hydrophobe substitution level and polymer concentration on the phase behavior and on the membrane properties of the surfactant membrane solutions. The variation of the elastic constant, κ , and compression modulus, \bar{B} , of the membranes as a function of added polymer concentration is determined by small angle neutron and x-ray scattering.

Experiments

Hydrophobically modified poly(sodium acrylate) with 0 to 3 mol% aliphatic chains containing 14 hydrocarbon units is made by grafting alkylamine in the presence of dicyclohexadecarbonimide onto a precursor polymer (polyacrylic acid) using a protocol developed by Illiopoulos [16]. The hydrophobic side chains are randomly distributed along the polymer backbone [17]. The molecular weight of the precursor polymers is 250,000, corresponding to 3400 repeat units. The surfactant membrane solution consists of pentaethylene glycol dodecyl ether ($C_{12}EO_5$), hexanol and brine, which was chosen because previous studies have determined the phase behavior of the neat system without polymer [18-19]. The molar ratio of hexanol to $C_{12}EO_5$ is kept constant (1.43 ± 0.02).

The study of phase diagrams was conducted in a thermal bath with samples contained in Parafilm® sealed vials. Phases were determined by visual inspection under a crossed polarizer. The lamellar phase is identified by its optical anisotropy: it is birefringent in transmitted light under crossed polarizer. The L_3 phase is optically clear and isotropic. The two coexistent lamellar phases, $L_{\alpha 1}/L_{\alpha 2}$ create a turbid mixture under a natural light and shows an interface between two birefringent phases after centrifugation. For samples close to the phase boundary, centrifugation and optical microscopy were used to determine the phase behavior of the solution.

Small angle neutron scattering experiments were performed at the Laboratory Leon Brillouin (Orphee reactor, Central d'étude de Saclay, France) on the neutron lines PACE and PAXE. The non-polarized neutron wavelengths were selected at 5, 8 and 12 Å ($\Delta\lambda/\lambda$ =about 3 %) while the two dimensional detector was kept at distances 1, 3.2 and 4 meters from samples. The wave vector range varied from 6×10^{-3} to

$3.5 \times 10^{-1} \text{ \AA}^{-1}$. Samples were held in 1 or 2 mm quartz cells. Relative scale spectra are obtained with respect with H_2O .

Results and Discussion

Phase Behavior. The phase diagram of the reference solution, $\text{C}_{12}\text{EO}_5/\text{C}_6\text{OH}/\text{brine}$ (0.1 M NaCl) over the temperature ranges from 5 °C to 60 °C is shown in Figure 1. Membrane volume fraction ϕ is defined as the ratio of the volume of surfactant plus alcohol to total volume of the solution. A broad monophasic L_α domain exists at room temperature for a membrane volume fraction of 6.2 % or higher, corresponding to a maximum interlamellar distance of order of 400 Å. The L_3 phase starts at a membrane volume fraction of 5.9 %. The system phase separates into a lamellar phase and an isotropic phase when the membrane volume fraction is lower than 5.9 %. Compared to the phase diagram of the binary system, $\text{C}_{12}\text{EO}_5/\text{H}_2\text{O}$ [15], all phase transition temperatures are shifted to lower values by roughly 50 °C.

A minimum amount of hydrophobic side chains is required to confine the polysoap in the membrane solution (Fig.2). Polymer is not soluble in the membrane mesophases when the hydrophobe substitution level is equal to or less than a 0.22 mol% at fixed polymer backbone molecular weight of 300,000. Consequently, a phase separation leads to a surfactant-rich membrane phase and a polymer-rich isotropic phase, even for very dilute membrane solutions. Polymer confinement in the membrane solution is not favored since the polymer loses conformational entropy. In contrast, when the hydrophobe level is higher than 0.7 mol %, the polysoap can be solubilized both in the lamellar phase L_α and the sponge phase L_3 . The critical hydrophobe substitution level is between 0.22 and 0.7 mol %. For the HM-polymer system hydrophobic interaction energy balances the reduction of entropy due to confinement. The hydrophobic side chains along the polymer backbone aggregate with hydrophobic species in aqueous, e.g., mixed micelles formed by hydrophobic side chains with surfactants [20-24]. The exchange energy for a CH_2 from a hydrocarbon environment to an aqueous environment is 1.8 $\text{K}_\text{B}\text{T}$ [25]. The hydrophobic side chains of the polymers anchor into the bilayers, forming polymer-coated membranes. Intra- or inter-polymer aggregation among hydrophobic groups is also possible in the solution. At this time we can not estimate the fraction of hydrophobes associated with the membrane relative to the hydrophobes associating in solution.

With the polymer inclusion, two new phases are observed (Fig. 3). They are two coexisting lamellar phases $L_{\alpha 1}/L_{\alpha 2}$ at high membrane concentration, and L_α' phase at low membrane concentrations adjacent to the lamellar domain. The L_α' solution is optically isotropic. Unlike lamellar phase, L_α' solution is not birefringent at rest, however, it exhibits birefringence under shear. The border between L_α and L_α' is determined by this difference in birefringence behavior. The L_α' solution has a higher viscosity than that of lamellar solution, especially for the solution close to the phase transition. A maximum turbidity exists during dilution, but no phase separation is observed under a microscope or after centrifugation. The flow birefringence gradually disappears upon to further dilution after the maximum turbidity is reached. The behavior of L_α' phase is similar to that of a vesicle phase reported by several groups

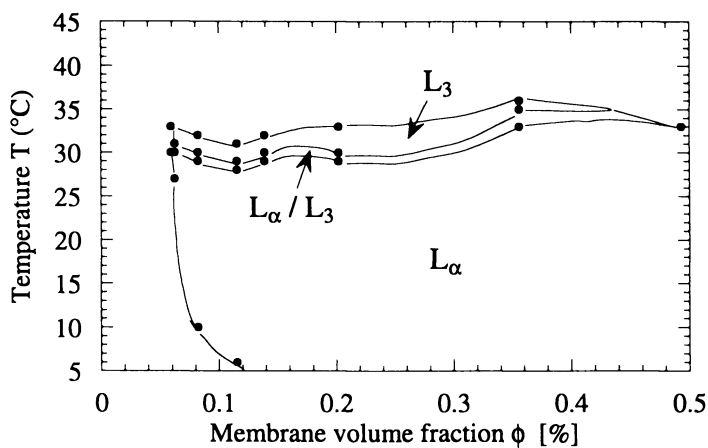


Figure 1. Phase diagram of reference system ($C_{12}EO_5/C_6OH/brine$).

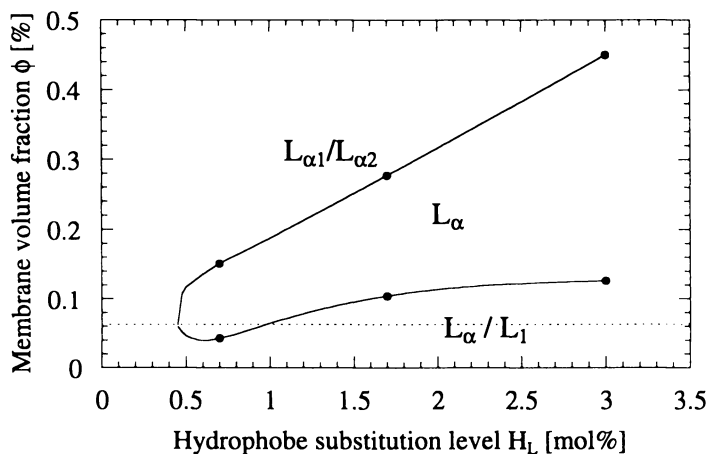


Figure 2. Hydrophobe substitution level effect on monophasic L_α solution at fixed polymer concentration $C_p = 0.2$ wt%, temperature $T = 25$ °C. The dashed line is low L_α boundary for reference solution.

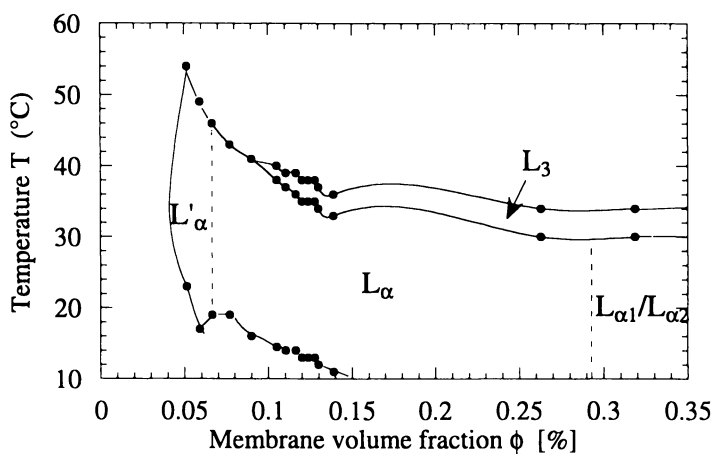


Figure 3. Phase diagram of HMPA doped membrane solution. Polymer concentration $C_p = 2$ wt%, substitution level $H_1 = 3$ mol%.

[26-29]. The transition between L_{α} and L_{α}' is also studied using SANS [30]. The results show that the L_{α}' phase is a membrane phase that is different from the lamellar phase. The difference may be related to a curvature change, for example vesicles formed from the membrane solution. Further study is required to fully characterize the L_{α}' phase. The $L_{\alpha_1}/L_{\alpha_2}$ solution is cloudy or turbid and separates into two macroscopic phases after centrifuged for an hour. Under neutron scattering, the $L_{\alpha_1}/L_{\alpha_2}$ solution shows two Bragg peaks reflecting two interlamellar distances.

The polymer concentration and hydrophobe substitution level determines the monophasic lamellar boundary (Fig.4). The area of the monophasic lamellar regime is reduced with polymer concentration at all substitution levels as has been reported by others [9,31]. The calculated phase diagrams for Helfrich-stabilized lamellar phases show that the two phases region increases with increasing bending modulus, κ . As we will see below, this prediction is consistent with our experimental results that show an increase in κ with polymer concentration. Higher polymer concentrations are accepted by the lamellar phase at lower hydrophobe levels (Fig.4). With HMPA-3 (3 mol % substituted polysoap), phase separation occurs when the polymer concentration is higher than 4.5 wt%. The limits of miscibility are shifted to concentrations of polymer of 6.5 wt% and 10.5 wt% for 2 mol% and 1 mol% substituted polymer (HMPA-2 and HMPA-1), respectively.

Membrane Properties. The effect of polymer on the elastic properties of the membranes is studied using scattering techniques. The scattering intensity from a lamellar phase produces a power law singularity of the Bragg peak, $I(q) \propto |q-q_0|^{-1+\eta}$, where the exponent η is defined in terms of the smectic elastic constants by Caille et al [32]:

$$\eta = \frac{k_B T q_0^2}{8\pi \sqrt{K \bar{B}}}$$

Where K is the smectic curvature modulus which is the ratio of membrane elastic constant, κ , to period spacing, d , (i.e. $K=\kappa/d$), reflecting the rigidity of single bilayer; \bar{B} is the layer compression modulus related to the bilayer/bilayer interactions. Figure 5 is a neutron scattering spectrum for HMPA-3 coated membranes with different polymer concentration at a fixed membrane volume fraction ($\phi=20\%$). The normalized Bragg peaks of the lamellar solution become narrower with growing polymer concentration (Fig. 5). This implies that the product $K\bar{B}$ increases with polymer addition. Also the diffuse scattering at small angles is reduced with polymer concentration. This indicates that the strength of the inter-membrane interactions increases with polymer concentration since the scattering intensity at low angle is inversely proportion to \bar{B} .

The variation of the elastic constant with polymer concentration is calculated using a theory relating the excess area of the membrane to its rigidity [33]. In a perfect one-dimensional stack of membranes, a simple dilution law, $d=\delta/\phi$, is followed. However, the fluctuating-membrane systems investigated in this study generate the excess area in a lamellar phase, arising from undulations. The projected area is smaller than that estimated by a one-dimensional model. Therefore, the interlamellar distance,

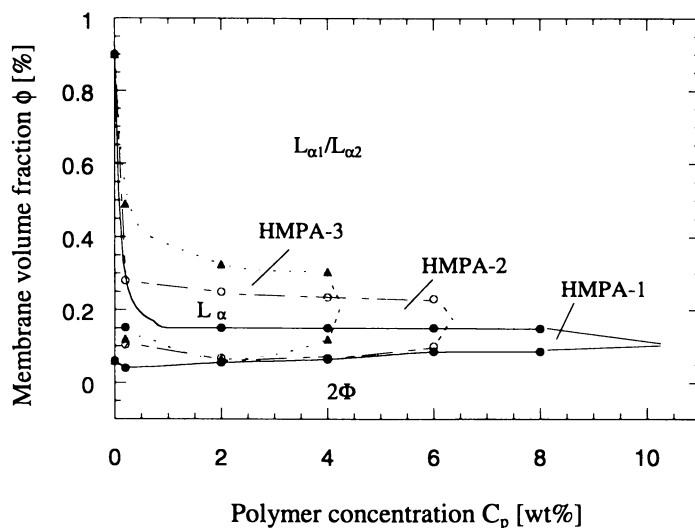


Figure 4. Polymer structure and concentration effect on the phase behavior of polymer doped membrane solutions. (Temperature = 25 °C).

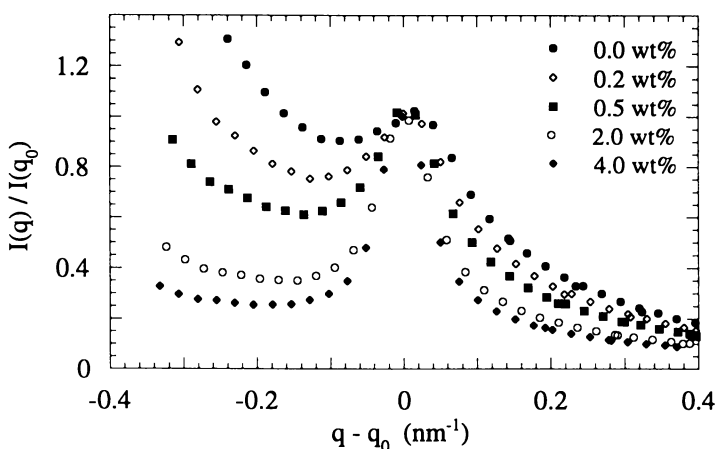


Figure 5. Normalized neutron scattering data of membrane solutions with different polymer concentration. Polymer concentration is indicated in the figure, membrane volume fraction $\phi = 20\%$, hydrophobe substitution level $H_1 = 3 \text{ mol}\%$. (Reproduced with permission from reference 14. Copyright 1998 American Physical Society.)

d , which also depends on the membrane bending modulus κ , is given by the following relationship with δ and ϕ [33]:

$$\frac{d\phi}{\delta} = 1 + \frac{1}{4\pi k} \ln \left[\frac{\delta}{\phi b} \sqrt{\frac{32k}{3\pi}} \right]$$

where b is a microscopic cutoff length. Based on this equation, variation of bending modulus can be monitored by simply measuring the interlamellar distance if membrane thickness is known. The value of δ is extracted from the high- q region of the neutron scattering spectra (Figure 6). From the peak position given by $\sin^2(q\delta/2)$, a membrane thickness $\delta = 24 \pm 2 \text{ \AA}$ is obtained. Membrane thickness is the same in the L_{α} and L_3 phases with different polymer concentrations, as shown in Figure 6. The variation of interlamellar distance, d , may also arise from the defect in lamellar structure [34]. However, the model developed by Nallet et al [35] for lamellar phase, $I(q) = q^{-2}P(q)S(q)$, is in good agreement with the experimental data [30]. It indicates that the effect of defects on variation of interlamellar spacing is not a dominant factor for this system. Hence the membrane elastic constant κ can be considered the only factor determining the interlamellar distance, since the membrane volume fraction is kept constant ($\phi = 20\%$). We show in Fig. 7, the relative elastic constant κ_r/κ_0 as a function of polymer concentration, where κ_0 is the elastic constant of the reference system. The relative elastic constant increases linearly with polymer concentration at low concentrations, then, appears to level off at a polymer concentrations above 2 wt%. The elastic constant almost doubles when polymer concentration increases from 0 to 4 wt%.

Both the elastic constant, κ , and the smectic compression modulus, \bar{B} , increase with polymer concentration (Figs. 5 and 7). This indicates that the polymer contributes to both inter- and intra-membrane. A large \bar{B} means a stiffening of the interlayer interaction potential. For a potential which is solely due to the steric Helfrich undulation interactions, the smectic modulus decreases with membrane stiffness $\bar{B} \sim 1/\kappa$. However, we find that κ increases with polymer concentration as does \bar{B} (Fig. 7). We conclude that the embedding of polymer in our system not only modifies the elastic properties of the membranes but also contributes to the inter-membrane potential.

Summary

In this study, we have demonstrated that polymer structure, polymer concentration and membrane volume fraction are determinate factors governing the phase behavior and bilayer membrane properties of the surfactant/polymer mixture. When the size of the polymer is of same order of the bilayer spacing, the presence of a critical hydrophobe substitution along the polyacrylate-based backbone is necessary to insert the polymer into bilayer stack. The hydrophobic anchoring groups associate with the lyotropic bilayer, therefore allowing for confinement. The anchoring polymer induces two new phases, a vesicle-like phase and two coexisting lamellar phases $L_{\alpha 1}/L_{\alpha 2}$. Moreover, the presence of the polymer increases the bending elastic modulus, κ , and compression modulus, \bar{B} .

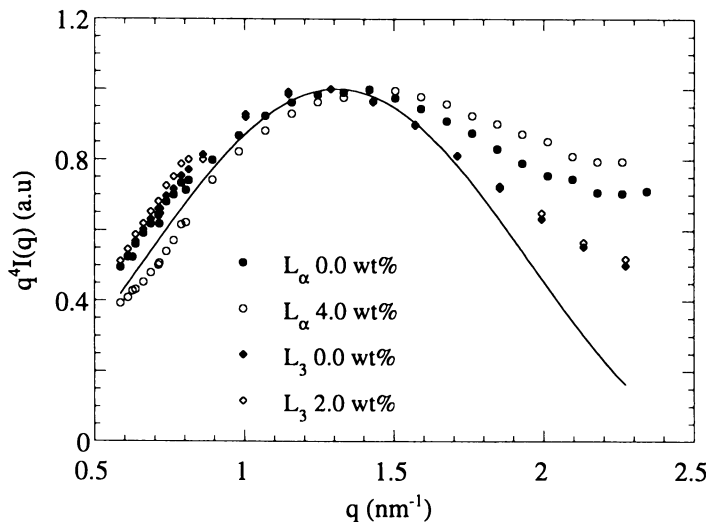


Figure 6. Large- q behavior of $q^4 I(q)$ in arbitrary units, showing one oscillation from which we extract the bilayer thickness $\delta = 2.4 \pm 0.2 \text{ nm}$. The fitting line is the function $\sin^2(q\delta/2)$. (Reproduced with permission from reference 14. Copyright 1998 American Physical Society.)

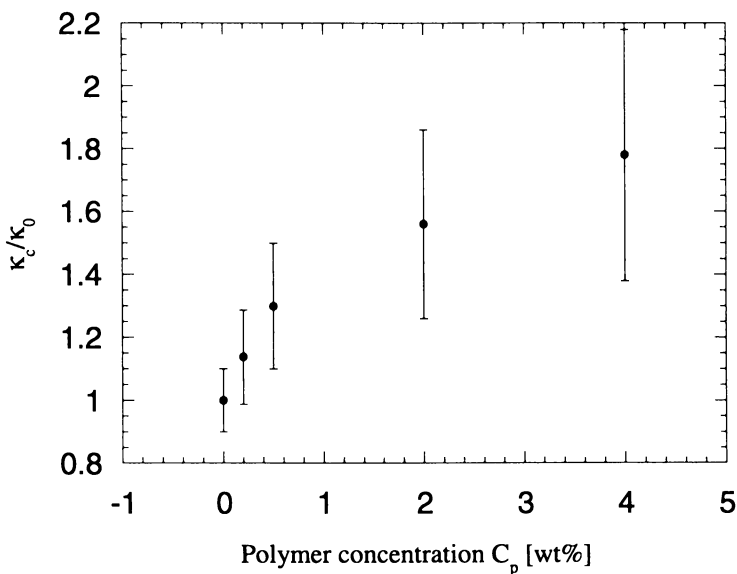


Figure 7. Polymer concentration effect on the membrane elastic constant. Membrane volume fraction $\phi = 20\%$, hydrophobe substitution level $H_f = 3 \text{ mol}\%$. (Reproduced with permission from reference 14. Copyright 1998 American Physical Society.)

References

1. C. Ligoure, G. Bouglet, and G. Porte, *Phys. Rev. Lett.* **1993**, *71*, 3600
2. H. Bagger-Jorgensen, U. Olsson and I. Iliopoulos, *Langmuir* **1995**, *11*, 1934
3. Bagger-Jorgensen, U. Olsson, I. Iliopoulos and K. Mortensen, *Langmuir* **1997**, *13*, 5820
4. K. Løyen, I. Iliopoulos, R. Audebert and U. Olsson, *Langmuir* **1995**, *11*, 1053
5. H. Bagger-Jorgensen, U. Olsson and I. Iliopoulos, *Langmuir* **1995**, *11*, 1934
6. V. Rajagopalan, U. Olsson and I. Iliopoulos, *Langmuir* **1996**, *12*, 4378.
7. B. Deme, M. Dubois, T. Zemb and B. Cabane, *J. Phys. Chem.* **1996**, *100*, 3828.
8. R. Lipowsky, *Europhys. Lett.* **1995**, *30*, 197
9. M. F. Ficheux, A.M. Bellocq and F. Nallet, *J. Phys. II France*, **1995**, *5*, 823.
10. E. Z. Radlinska, T. Gulik-Krzywicki, F. Lafuma, D. Langevin, W. Urbach, S. E. Williams, and R. Ober, *Phys. Rev. Lett.* **1995**, *74*, 4237.
11. E. Z. Radlinska, T. Gulik-Krzywicki, F. Lafuma, D. Langevin, W. Urbach and S. E. Williams, *J. Phys. II France* **1997**, *7*, 1393
12. J. T. Brooks, C. M. Marques, and M. E. Cates, *Europhys. Lett.* **1991**, *14*, 713
13. G. Bouglet, C. Ligoure, A.M. Bellocq, E. Dufourc, and G. Mosser, *Phys. Rev. E*, **1998**, *57*,1
14. Y. Yang, R. Prudhomme, K. M. McGrath, P. Richetti and C. M. Marques, *Phys. Rev. Lett.* **1998**, *80*, 2729
15. R. Strey et al., *J. Chem. Soc. Faraday Trans.* **1990**, *86*, 2253
16. T. K. Wang, I. Iliopoulos, R. Audebert, *Polym. Bull.* **1988**, *20*, 577
17. I. Iliopoulos, T. K. Wang and R. Audebert, *Langmuir* **1991**, *7*, 617
18. R. Strey and M. Jonstromer, *J. Phys. Chem.* **1992**, *96*, 5993
19. E. Freyssingéas, F. Nallet and D. Roux, *langmuir*, **1996**, *12*, 6028
20. A. J. Dualé and C. A. Steiner, *Macromolecules* **1990**, *23*, 251
21. R. Tanaka, J. Meadows, P. A. Williams and G. O. Phillips, *Macromolecules*, **1992**, *25*, 1304
22. I. Iliopoulos, T. K. Wang and R. Audebert, *Langmuir*, **1991**, *7*, 617
23. B. Nyström, H. Walderhaug, F. K. Hansen and B. Lindman, *Langmuir*, **1995**, *11*, 750
24. L. Piculell, F. Guillemet and K. Thuresson *Advances in Colloid and Interface Science*, **1996**, *63*, 1
25. T. Annable, R. Buscall, R. Ettelaie, and D. Whittlestone, *J. Rheol.* **1993**, *37*, 695
26. M. H. G. M. Penders and R. Strey, *J. Phys. Chem.* **1995**, *99*, 6091
27. R. Strey, *Ber. Bunsenges. Phys. Chem.* **1996**, *100*, 182
28. H. Hoffmann, U. Munkert, C. Thunig, and M. Valiente, *J. Colloid and Interface Sci.* **1994**, *163*, 217
29. P. Herve, D. Roux, A. M. Bellocq, F. Nallet and T. Gulik-Krzywicki, *J. Phys. II France*, **1993**, *3*, 1225
30. Y. Yang, R. Pud'homme, A. Zirkel, C. M. Marques, and P. Richetti, prepared for *langmuir*
31. K. Zhang and P. Linse, *J. Phys. Chem.* **1995**, *99*, 9130

32. A. Caille, C.R. Jeb. Sean, *Acad. Sci.* **1972**, B274, 1733
33. D. Roux, F. Nallet, E.Freyssingeas, G. Porte, P. Bassereau, M. Skouri and J. Marignan, *Europhysics Letters*, **1992**,17 (7), 575
34. S. T. Hyde, *Langmuir*, **1997**, 13 842
35. F. Nallet, R. Laversanne and D. Roux, *J. Phys. II France*, **1993**, 3, 487